N87-26424

DESIGN STUDY OF LARGE AREA 8 cm x 8 cm WRAPTHROUGH CELLS FOR SPACE STATION

George F.J. Garlick and David R. Lillington
Spectrolab, Inc.
Sylmar, California

This paper reports on the design of large area silicon solar cells for the projected NASA Space Station. It is based on the NASA specification for the cells which calls for an 8 cm x 8 cm cell of wrapthrough type with gridded back contacts. The Beginning of Life (BOL) power must be 1.039 watts per cell or larger and maximum End of Life (EOL) after ten years in the prescribed orbit under an equivalent 1MeV electron radiation damage fluence of $5x10^{13}$ e/cm^2. On orbit efficiency is to be optimized by a low thermal absorptance goal (thermal alpha) of .63.

Within the above specification there is some latitude left to the designer in such factors as choice of cell type e.g. base resistivity, thickness and presence or absence of a back surface field (BSF) and planar or textured front surface. Emphasis is also placed on fabrication cost and power/weight ratio.

The design study was carried out under Task I of NASA contract NAS3-24672. This task covered a period of three months. It combined detailed computer modeling with input of actual data from previous cell diagnostics for factors such as radiation hardness, antireflection coating optimization and thermal alpha tests.

The relatively novel features of such cells are their large size, gridded back contacts and wrapthrough system. In this study, computation is extended beyond the required limits for completeness. For example cell performance was considered out to fluences of 10^{14} and 10^{15} 1 MeV e/cm^2 and the effects of front and back surface passivations were found.

THE DESIGN STUDY

Choice of Cell Type

Choice of cell type is strongly influenced by the radiation damage (EOL) after $5x10^{13}$ 1 MeV e/cm^2 fluence. However, this is small enough to include BSF cells in the considerations and also cells with lower base resistivities. Thus we considered cells of both 2 and 10 ohm-cm resistivities and in relation to manufacturing costs we considered both thin (4 mil) and thick (8 mil) cells. As shown below these choices can yield cells which lie above the minimum BOL power requirements. Textured and planar front and back surfaces were also considered. The various possibilities are shown schematically in Figures 1a through 1d.

The Modeling Basis

Computer programs have been developed which are based on the accepted analytical equations for cell transport processes. Typical parameters entered into the programs for cells are given in Table 1. The emitter characteristics are very similar to those optimized for space cells by Spectrolab after many years of experience. Variables of particular importance are the front and back surface recombination velocities. The usual front surface value is 5.10^4 cm/s when the emitter is thin but

for thicker emitters (deeper junctions) this velocity becomes critical and must be reduced to around 1000 cm/s. In the case of the back surface without BSF we find that the P-silicon to aluminum contact has a recombination velocity of about 1500 cm/s. When a BSF is present, best values are 10 cm/s but having in mind the use of a boron diffused or implanted BSF considered for the Space Station cells we adopted a more conservative estimate of 100 cm/s.

With respect to the antireflection coatings on front and back surfaces we again used data from previous work adding to them the analysis of the situation where a passivation layer of relatively low refractive index underlies the A.R. coating. The A.R. reflection spectra of actual cell types and also those computed for cells with the added passivation layers were used in the cell performance computations.

In order to maximize cell power when gridded front and back contacts are used the series resistance must be minimized. Spectrolab has computer models which, given a specific grid geometry, carry out optimization analysis to minimize resistive losses. Consideration of deeper junctions was included since these will reduce the sheet resistance of the emitter layer. However, as shown later and mentioned above, there is then a critical need to lower front surface recombination velocities by passivation.

Modeling Results

In this section we present the results of modeling for the cells at 25°C. These are then used in the next section to determine on orbit performance.

Series Resistance Minimization

Figure 2 gives the important parameters for the model which gives optimum grid geometry for minimum series resistance. They comprise the grid line dimensions and grid spacing, sheet resistance of the emitter region and ohmic bar dimensions. Grid line tapering is also taken into account. Effects of base and gridded back structure are also included. The latter is not as critical as the front grid structure.

To use the results for each design of wrap structure a value for series resistance so derived is used in obtaining an I-V curve for each cell and so cell power is found. The grid analysis involves an iterative nodal approach along each grid line. A favorable set of dimensions is a grid height of 10μM, a width of 25μM (average along taper) and a grid spacing of 800μM. A similar set of dimensions was chosen for the back contact grid system positioned to match the front structure.

Figure 3 shows one possible approach to the front and back contact designs for an 8 cm x 8 cm cell. Eight P+ contacts are provided with 4 N+ contacts. The series resistance for each of various cell types are later included in the cell performance assessment in Table 3. Other wrapthrough options such as small laser drilled holes which may reduce the wrapthrough contact area and shunt leakage losses are also currently being considered for the cell design.

Input Power Optimization

Optimization of input power is critically dependent on the attainment of minimum reflection of solar flux at the front surface by suitable antireflection coatings (A.R.) which may have to be deposited onto a passivation layer of lower refractive

index formed on the emitter surface. Programs exist at Spectrolab which, given the solar irradiance spectrum, the reflection spectrum of the silicon itself and the nature of any passivation layer, can by an iterative process determine the optimum thicknesses of dual A.R. layers of given materials. Figure 4 gives an illustration of their efficacy. A standard A.R. dual layer coating on top of a 100Å passivating silicon dioxide layer will greatly offset the A.R. performance. However, application of the programs gives adjusted A.R. coating thicknesses which can restore the performance.

Linked to the optimization of front surface A.R. coatings to minimize reflection across the active cell spectrum is the need to maximize transmission of the unwanted radiation through the back surface. In this way the thermal alpha for the cell is minimized. Figure 5 gives an empirical comparison of planar and textured cells with 'glassed' gridded back cells and A.R. coatings on both faces. The cells were 2 cm x 2 cm and boron was used as the BSF dopant where appropriate. The coverglass used was OCLI fused silica with a multilayer UVR coating on the backside and MgF_2 A.R. coating on the front side. The cells were glassed on the front side only. The excellent minimization of thermal alpha for the planar cells is very evident and is unaffected by the use of boron as a BSF dopant. The effects of these front and back surface reflection optimizations on cell peformance, particularly on orbit is brought out in Table 2.

Cell Performance Optimization

The reflection spectra of Figure 3 can be used together with the solar irradiance spectrum in the main cell computer programs to compute the operational parameters of the cells. The specifications required by NASA are for cells operating at 25°C and so the first five columns of data are for this case. However, it is important to determine what the "on orbit" cell performance will be and so using the thermal alpha value determined for each cell type from data such as those of Figure 5 we have calculated the on orbit temperature and then the cell efficiencies on orbit, by means of the formula:

$$T^4 = \frac{S(\alpha-\eta)}{\sigma(\varepsilon_1+\varepsilon_2)}$$

where S = radiant energy falling on cell equal to the solar constant for normal incidence,

α = solar absorptance of the incident surface or thermal alpha,
ε_1 = hemispherical emittance of front surface,
ε_2 = hemispherical emittance of back surface,
σ = Stefan's constant and
T = operating temperature of the cell in °K.

Figure 6 depicts the dependence of cell on orbit temperature on thermal alpha for a number of different cell photovoltaic efficiencies. Positions are indicated for different cell types chosen in our design study and for an ideal cell. It should be noted that the ideal thermal alpha is higher than the planar cell case. This is because perfect absorption is not attained over the cell active response spectrum in practice. Figure 7 gives other essential information namely the dependence of cell efficiency on temperature for various cell types and also indicates the temperature appropriate to each type as given by the respective thermal alpha value. These determinations enable us to compute the on orbit performance of the cells which is presented in the last two columns of Tables 2a and 2b.

From the results shown in Tables 2a and 2b it was possible to eliminate certain cell types from the list of possible candidates. It is clear, for instance, that sculptured cells, although providing a high efficiency at 25°C, currently have too high thermal alpha to be useful in a planar array since the on orbit operating temperature is too high. This results in the 'on orbit' efficiency being lower for sculptured cells than for planar cells. However, there is some evidence that the thermal alpha of gridded back sculptured cells may be significantly improved by further process modification. This work continues to be supported under NASA LeRC contract NAS3 24672 but will not be reported on here.

Further, more detailed modeling was performed on planar cell typoes considered to be most promising for use on Space Station given present thermal alpha data. These types were 2 ohm-cm 8 mil planar, 2 ohm-cm 4 mil planar BSF, 2 ohm-cm 8 mil planar BSF, and 10 ohm-cm 4 mil planar BSF. Additionally detailed grid modeling was performed on these cell types to differentiate between wraparound (WA) and wrapthrough (WT) cell types since there are some series resistance implications. The 25°C and on orbit (approximately 20°C) data for these cells is shown in Table 3. We discuss the tabled results below.

DISCUSSION

From the results of our modeling shown in Table 3 it is apparent that the choice of cell most suitable for Space Station is determined to some extent by the projected lifetime of the cell. If a 10 year lifetime is considered, corresponding to a fluence of approximately 5.10^{13} 1 MeV electrons cm^{-2}, then the 2 ohm-cm planar 4 mil cell with boron BSF has an EOL efficiency significantly greater than the 8 mil 2 ohm-cm planar non-fielded part. This is because the degradation in diffusion length at 5.10^{13} 1 MeV electrons cm^{-2} is not sufficient to have significantly reduced the effect of the BSF. At 10^{14} 1 MeV fluence (corresponding to 20 year life) the effect of the BSF is almost eliminated and the efficiencies of the fielded and non-fielded parts begin to converge. Generally the 10 ohm-cm 4 mil part does not maintain power to EOL as well as the 2 ohm-cm parts. We believe this is due to the higher doping concentration in the 2 ohm-cm substrate which suppresses I_{01} (the first diode saturation current). Based on current radiation damage coefficient data for 2 ohm-cm silicon we do not see a catastrophic fall in diffusion length with radiation which would otherwise increase I_{01}.

In terms of cell configuration it is clear that the wrapthrough design consistently yields higher values of efficiency than the wraparound design. This is a direct result of reduced resistive losses in the grids due to the shorter average distance that current has to flow to the ohmic current collection bar. This is evidenced by the value of R_s shown in column 3 of Table 3.

The decision whether or not to produce a 4 mil product for Space Station (vs 8 mil) is predicated largely on yield arguments. In efficiency terms there appears to be little difference between a 2 ohm-cm 4 mil, K6 wrapthrough cell and a 2 ohm-cm 8 mil wrapthrough cell. For instance at BOL the efficiencies are 14.7% and 14.5% for the 4 mil and 8 mil cells respectively, whilst at 1E14 1 MeV electron fluence the efficiencies are 13.5% and 13.1% respectively. Since cost will be a major issue for the Space Station cell and since yield is certain to be higher on the 8 mil cell, it was decided jointly by NASA and Spectrolab, with input from other aerospace companies, to pursue the 8 mil K6 planar cell in the Task II engineering development phase.

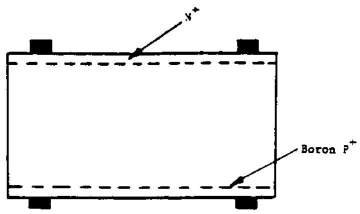

Figure 1a: SCHEMATIC OF GRIDDED P^+ BACK K6 CELL WITH PLANAR FRONT AND BACK

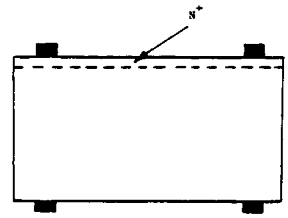

Figure 1c: SCHEMATIC OF GRIDDED BACK K4 CELL WITH PLANAR FRONT AND BACK

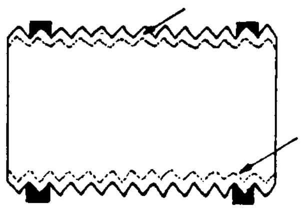

Figure 1b: SCHEMATIC OF GRIDDED P^+ BACK K7 CELL WITH SCULPTURED FRONT AND BACK

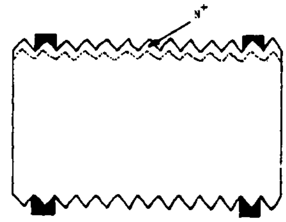

Figure 1d: SCHEMATIC OF GRIDDED BACK K5 CELL WITH SCULPTURED FRONT AND BACK

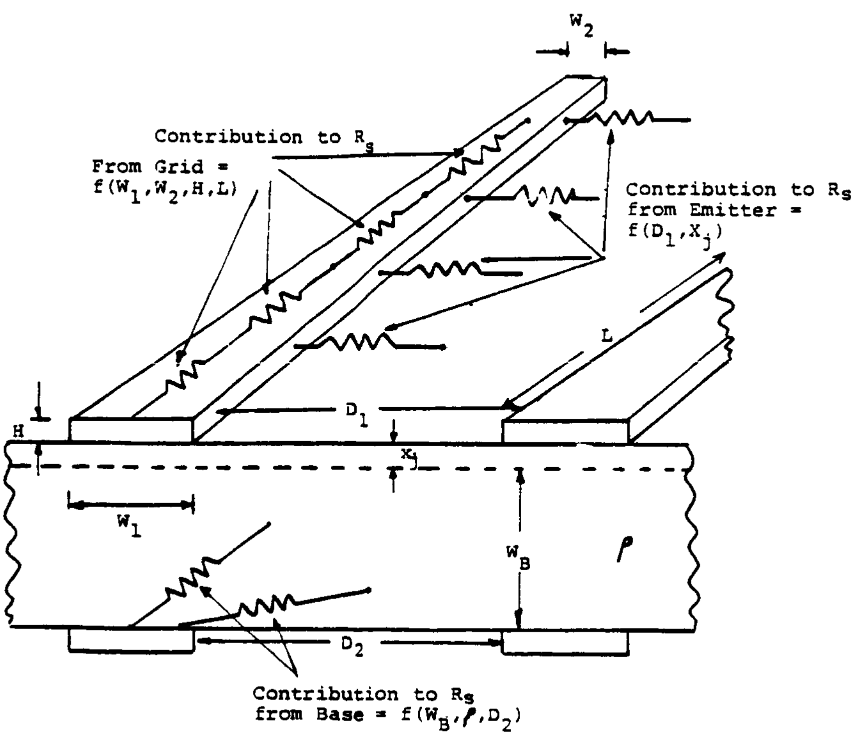

Figure 2: IMPORTANT PARAMETERS CONTROLLING GRID LINE OPTIMIZATION

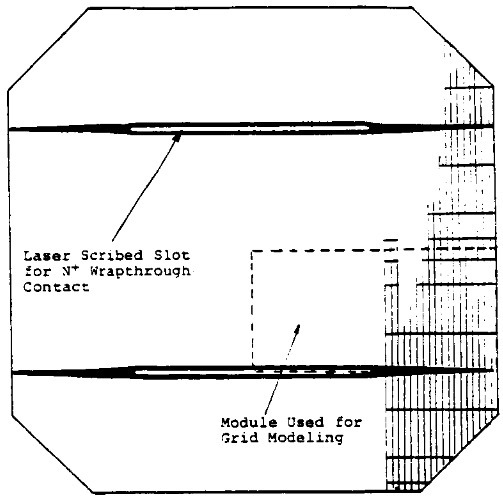

FIGURE 3a: PROPOSED FRONT CONTACT DESIGN FOR 8 CM X 8 CM WRAPTHROUGH CELL

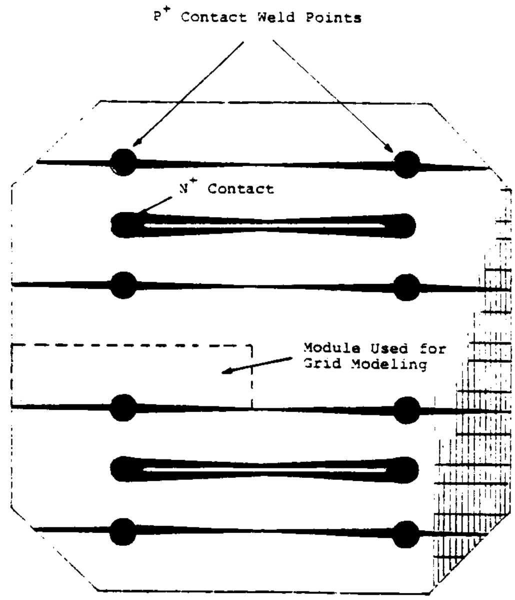

FIGURE 3b: PROPOSED BACK CONTACT DESIGN FOR 8 CM X 8 CM WRAPTHROUGH CELL

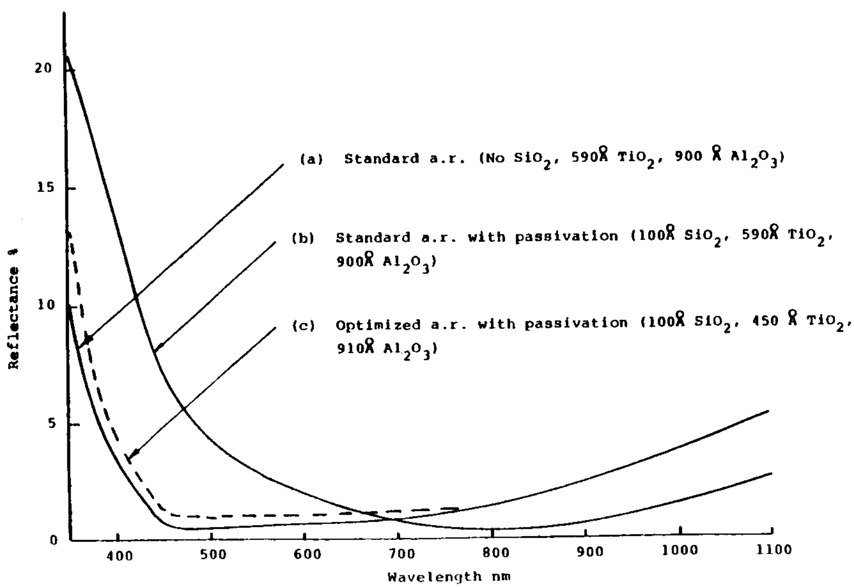

FIGURE 4: COMPUTED SPECTRAL REFLECTANCE FROM DC 93500 COVERED K4 SURFACE FOR DIFFERENT A.R. COATING AND PASSIVATION OXIDE THICKNESSES

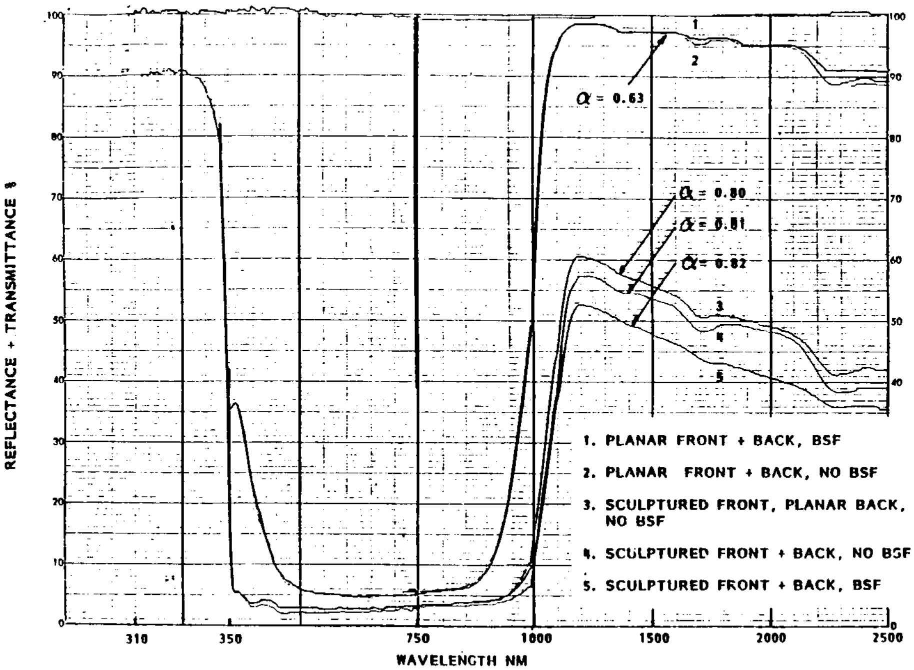

FIGURE 5: MEASURED SPECTRAL REFLECTANCE + TRANSMITTANCE OF GLASSED GRIDDED BACK CELLS WITH DUAL A.R. COATING BOTH SIDES

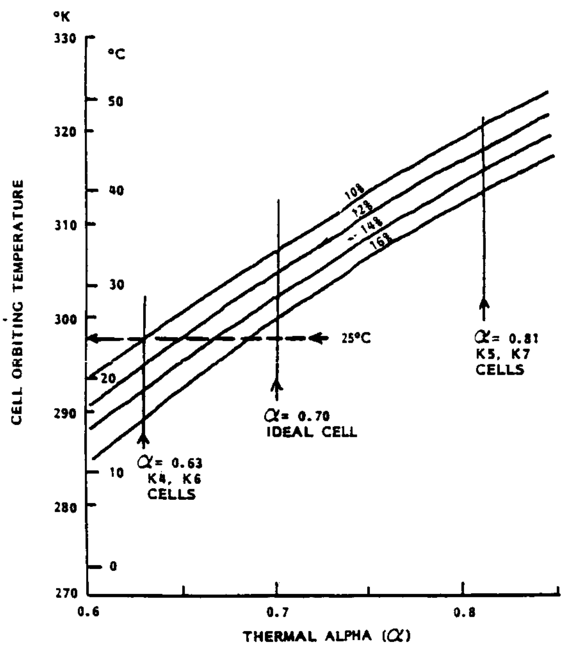

FIGURE 6: CALCULATED CELL ORBITING TEMPERATURE AS A FUNCTION OF THERMAL ALPHA AND EFFICIENCY. OPERATING POINTS FOR IDEAL CELL AND GRIDDED BACK K4, K5, K6, AND K7 CELLS ARE ALSO SHOWN

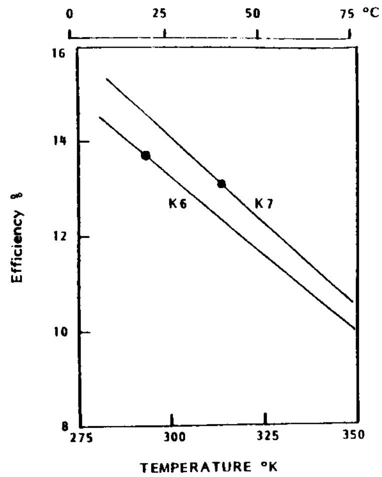

Fig 7a

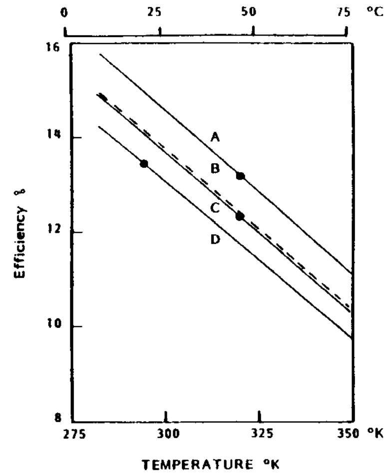

Fig 7b

Fig 7a & 7b COMPUTED DEPENDENCE OF BOL CELL EFFICIENCY ON TEMPERATURE

Fig 7a 10 OHM-CM, 8 MIL, BSF K6 and K7 CELLS (S_{back} = 100 CM SEC^{-1})

Fig 7b 2 OHM-CM CELLS: A - 4 MIL K7, B - 4 MIL (BROKEN LINE)
C - 8 MIL K5, D - 8 MIL K4

o DENOTES ON ORBIT OPERATING TEMPERATURE AND EFFICIENCY BASED ON MEASURED THERMAL ALPHA (See Fig 5)

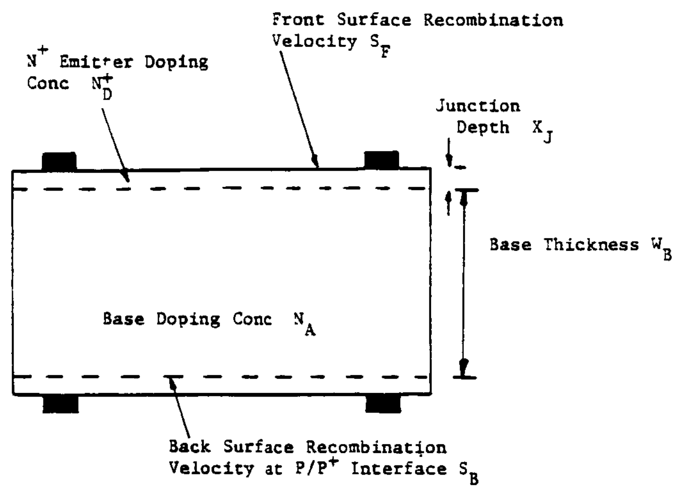

PARAMETERS USED IN MODELING OF TABLE 1

Emitter	10 Ohm-cm Base	2 Ohm-cm Base
X_J = 0.15 microns	L_N = 700 microns	L_N = 300 microns
L_P = 2.38 microns	D_N = 35 cm^2 S^{-1}	D_N = 28 cm^2 S^{-1}
D_P = 1.74 cm^2 S^{-1}	S_B = 100 cm S^{-1}	S_B = 100 cm S^{-1}
S_F = 5E4 cm S^{-1}	N_A = 1.4 E15 cm^{-3}	N_A = 7.5E15
N_D^+ (mean) = 5E18 cm^{-3}		

TABLE 1: SCHEMATIC OF SOLAR CELL STRUCTURE SHOWING MOST IMPORTANT MODELING PARAMETERS AND THOSE VALUES USED IN OBTAINING PRELIMINARY RESULTS OF TABLE 1.

Cell Type	Fluence ϕ(e cm^{-2})	V_{oc} mV	J_{sc} mA cm^{-2}	Effy @ 25°C %	P/P_o	FF*	Thermal Alpha	Effy On Orbit %
2 ohm-cm, 8 mil, K4	0	595.0	38.3	13.1	1	0.780	0.63	13.5
" "	5 x 10^{13}	583.0	37.6	12.5	0.96	0.775	0.63	12.8
" "	1 x 10^{14}	576.1	37.1	12.2	0.93	0.773	0.63	12.6
2 ohm-cm, 8 mil, K5	0	583.3	42.1	14.0	1	0.770	0.81	12.5
" "	5 x 10^{13}	571.3	41.3	13.2	0.96	0.761	0.81	12.0
	1 x 10^{14}	564.3	40.8	13.0	0.93	0.763	0.81	11.6
2 ohm-cm, 4 mil, K6	0	618.6	38.6	13.8	1	0.783	0.63	14.1
" "	5 x 10^{13}	596.3	38.0	13.0	0.94	0.777	0.63	13.2
" "	1 x 10^{14}	585.5	37.6	12.6	0.91	0.774	0.63	12.9
2 ohm-cm, 4 mil, K7	0	606.7	42.2	14.7	1	0.774	0.81	13.2
" "	5 x 10^{13}	584.4	41.6	13.8	0.94	0.768	0.81	12.3
" "	1 x 10^{14}	573.5	41.1	13.3	0.91	0.763	0.81	12.0

*Assumes series resistance = 800 mohm-cm^2

Table 2a: Computed AMO Cell Characteristics of Different Cell Types as a Function of 1 MeV Electron Fluence Using Reflectance and Transmittance Data of Figure 5.

Cell Type	Fluence ϕ(e cm^{-2})	V_{oc} mV	J_{sc} mA cm^{-2}	Effy @ 25°C %	P/P_o	FF*	Thermal Alpha	Effy On Orbit %
10 ohm-cm, 8 mil, K6	0	592.4	39.6	13.4	1	0.776	0.63	13.7
" "	5 x 10^{13}	553.6	38.8	12.1	0.90	0.764	0.63	12.6
" "	1 x 10^{14}	541.3	38.2	11.6	0.87	0.761	0.63	11.9
10 ohm-cm, 8 mil, K7	0	580.9	43.7	14.4	1	0.767	0.81	12.9
" "	5 x 10^{13}	541.7	42.8	12.9	0.90	0.755	0.81	12.0
" "	1 x 10^{14}	529.4	42.1	12.4	0.86	0.751	0.81	11.6
10 ohm-cm, 4 mil, K6	0	599.4	38.8	13.4	1	0.778	0.63	13.7
" "	5 x 10^{13}	565.8	38.5	12.3	0.92	0.767	0.63	12.8
" "	1 x 10^{14}	557.6	38.2	11.9	0.89	0.763	0.63	12.5
10 ohm-cm, 4 mil, K7	0	587.6	42.5	14.2	1	0.770	0.81	13.0
" "	5 x 10^{13}	552.9	42.1	13.1	0.92	0.758	0.81	12.1
" "	1 x 10^{14}	539.4	41.8	12.6	0.88	0.753	0.81	11.7

*Assumes series resistance - 800 mohm-cm^2

Table 2b: Computed AMO Cell Characteristics of Different Cell Types as a Function of 1 MeV Electron Fluence Using Reflectance and Transmittance Data of Figure 5.

Table 3: Predicted AMO 25^{O}C and 'On Orbit' Performance of Selected Cell Structures with Optimized Grid Designs

Cell Type	Fluence ϕ(e cm^{-2})	R_s milliohm cm^{-2}	P_{max}W (25°C)	Effy (25°C)	FF (25°C)	Effy on Orbit (~20°C)
2 ohm-cm 8 mil K4 WA	0	504	1.09	13.4	0.80	13.8
	5×10^{13}	504	1.04	12.82	0.79	13.2
	1×10^{14}	504	1:01	12.5	0.79	12.8
2 ohm-cm 8 mil K4 WT	0	268	1.11	13.6	0.81	14.0
	5×10^{13}	268	1.06	13.0	0.81	13.4
	1×10^{14}	268	1.03	12.7	0.80	13.0
2 ohm-cm 4 mil K6 WA	0	454	1.13	14.2	0.80	14.5
	5×10^{13}	454	1.09	13.4	0.80	13.7
	1×10^{14}	454	1.05	12.9	0.79	13.3
2 ohm-cm 4 mil K6 WT	0	260	1.17	14.3	0.81	14.7
	5×10^{13}	260	1.10	13.5	0.81	13.9
	1×10^{14}	260	1.07	13.0	0.80	13.5
10 ohm-cm 4 mil K6 WA	0	619	1.10	13.5	0.79	13.8
	5×10^{13}	619	1.02	12.5	0.78	12.9
	1×10^{14}	619	0.98	12.0	0.77	12.4
10 ohm-cm 4 mil K6 WT	0	289	1.12	13.8	0.81	14.2
	5×10^{13}	289	1.04	12.8	0.80	13.2
	1×10^{14}	289	1.00	12.3	0.79	12.7

Total Cell Area 60.14 cm^2. WA = Wraparound. WT-Wrapthrough